

Collision Induced Dephasing in Fluorescence Quantum Beat of $\text{SO}_2(\tilde{\text{C}}^1\text{B}_2)^\dagger$

Min Zhang, Jun Han, Peng Liu, Don Muller, and Hai-Lung Dai*

Department of Chemistry, University of Pennsylvania, Philadelphia, Pennsylvania 19104-6323

Received: July 31, 2003; In Final Form: October 1, 2003

The collision-induced pure dephasing rate constant of a pair of coherently excited eigenlevels of SO_2 is measured. This represents the first measurement of a collision-induced pure dephasing constant for a molecule in gaseous phase. The pair of eigenlevels arises from the coupling of the $\tilde{\text{C}}(210)7_{16}$ level and an isoenergetic high vibrational level, 44877.52 cm^{-1} above the zero point, of the $\tilde{\text{X}}$ state. The pure dephasing cross sections measured for the three colliding partners He, Ar, and SO_2 at the temperature 4.8 K are respectively 26, 40, and 720 \AA^2 . All three pure dephasing cross sections are about a factor of 2 smaller than the corresponding depopulation cross sections. Comparison with the hard sphere and Lennard-Jones cross sections suggests that collision-induced dephasing involves more than hard sphere, repulsive forces.

I. Introduction

In the study of intramolecular and intermolecular dynamics such as energy redistribution, fluorescence decay following photon-induced molecular excitation has been explored extensively.^{1,2} In some unusual cases, periodic oscillation in fluorescence intensity, or quantum beat³ (QB), has been observed in the fluorescence decay. QB is not only a demonstration of the fundamental principles of quantum mechanics, it is also a unique phenomenon associated with intramolecular coupling. In the simplest case of a two coupled level system in the excited state, QB arises from simultaneous and coherent excitation of the two excited eigenlevels that derive their wave functions from coupling of two zeroth order levels—one “bright” and one “dark”. When the total fluorescence from both eigenlevels leading to the same set of lower levels is monitored, because the photons emitted from these coherently excited levels are indistinguishable, the fluorescence intensity follows the square of the sum of the evolving wave functions of the excited eigenlevels. In adding the eigenlevel wave functions coherently, constructive and destructive interactions of the wave functions occur leading to the oscillation of the bright and dark states wave functions. Quantum beats, which can also be generated through external magnetic/electric field induced intramolecular coupling, in fluorescence decay have been observed for molecules such as SO_2 ,^{4–6} NO_2 ,^{7,8} CS_2 ,⁹ acetylene,¹⁰ glyoxal,¹¹ pyrazine,¹² biacetyl,^{13,14} and even radicals such as HCCS.¹⁵

A unique usage of the observed QB is the access to the optically inaccessible dark states. For example, one such dark state is the highly vibrationally excited level in the electronic ground state. These levels are of critical importance to a wide range of topics ranging from mode- or bond-selective reaction,¹⁶ unimolecular dissociation,¹⁷ combustion,¹⁸ atmospheric chemistry,^{19,20} intramolecular vibrational relaxation,²¹ to collision energy transfer.^{22,23} The highly excited vibrational levels can be prepared by Franck–Condon pumping through dispersed fluorescence,²⁴ stimulated emission pumping,²⁵ internal conversion following electronic excitation,²⁶ single photon overtone excitation,²⁷ or chemical activation.²⁸ These methods, however,

are hard pressed for the preparation of a *single, highly excited* vibrational level in the energy region where the vibrational level density is high. The QB phenomenon though rare to find, on the other hand, offers a unique and effective way of accessing a single, highly excited level.⁴

Single, high vibrational levels of the electronic ground state can be accessed through excitation of optically bright states in coupling with the high vibration levels. For example, the dissociation rates of many high vibrational levels above the dissociation limit of formaldehyde have been measured through Stark field induced coupling of the target vibrational levels and the near isoenergetic, bright $\tilde{\text{A}}$ state levels.^{29,30} In SO_2 QB's observed in the $\tilde{\text{C}}^1\text{B}_2 \leftarrow \tilde{\text{X}}^1\text{A}_1$ transition region have been shown to arise from coupling between $\tilde{\text{X}}$ and $\tilde{\text{C}}$ states levels as the beat frequencies were shown to be unresponsive to the applied magnetic field.⁵ Xue et al. have used the QB of SO_2 in the $\tilde{\text{C}}^1\text{B}_2$ state region to measure the collision quenching cross section of a single, high rovibrational level at 44877.52 cm^{-1} above the zero point.⁴ The decay rate constants of eigenlevels, which are directly related to the zero-order level decay constants, can be obtained by the fluorescence QB decay as a function of pressure. The decay rate constant of the “bright” state can be measured from fluorescence decay of other $\tilde{\text{C}}^1\text{B}_2$ rovibronic levels that are not coupled. Subsequently, the decay constant of the “dark” high vibrational level of the electronic ground state can be obtained.

In the analysis of the collision effect on the QB decay, based on the nearly indiscernible difference between the overall fluorescence intensity decay rate and the decay rate of the oscillatory part of the intensity, it was assumed that the primary effect of collision is to depopulate the eigenlevels. Pure dephasing, i.e., the destruction of coherence without loss of population, of the two coherently excited levels is assumed to be negligible.

In general, in considering the time evolution of the fluorescence QB, we need to include both dephasing and depopulation of the coherently excited states.^{31–33} In the density matrix treatment of the simplest QB case of two coupled states, depopulation is described by the time decay behavior of the diagonal elements, while dephasing is the time dependence of the off-diagonal elements.³¹ The time evolution of the diagonal

* To whom all correspondence shall be addressed.

† Part of the special issue “Charles S. Parmenter Festschrift”.

and off-diagonal elements may be affected differently by collisions between bath molecules and the QB molecule.^{32,33} So far only a limited number of studies, experimental^{8,9,14} and theoretical,^{31–34} has considered the dephasing rate in quantum beats in molecular systems.

For atomic systems, such as the well characterized fluorescence QB decay following coherent excitation of Na D lines,³⁵ it is usually assumed that collision-induced pure dephasing rate is small in comparison with the depopulation rate. This assumption has been found to be consistent with the analysis of the observed QB decay. For molecular systems, Chang et al.'s work on biacetyl, where multiple level quantum beats have been observed, has been the only attempt to explicitly examine the dephasing rate in QB decay as a function of pressure.¹⁴ In that study the experimental measurements appear to indicate that the collision depopulation rate is faster than the pure dephasing rate.

Pure dephasing collisions are elastic—no energy exchange results. Another form of elastic collisions that may contribute to dephasing is “depolarization”, which has been studied in Zeeman QB.^{7,8} A Zeeman QB signal is caused by the alignment of the excited-state molecules along the laser polarization. Here, collision-induced dephasing may cause the loss of optical alignment of the excited molecules. Brucat and Zare have studied the depolarization of NO₂⁷ and showed that the rate of depolarization caused by collision is smaller than the rate of population removal by collision. Similarly a study on CS₂ has indicated that the depolarization of QB is pressure-dependent.⁹

In this paper, we examine the contribution of collision-induced dephasing to the decay of SO₂ QB. SO₂ is cooled in a supersonic jet, where the QB pattern can be clearly resolved without rotational congestion and is recorded as a function of the stagnation pressure. A model that includes both the dephasing and depopulation contributions to QB decay is used for analyzing the fluorescence QB decay. The collision cross sections of pure dephasing by several collision partners have been measured. Since the QB of SO₂ is the simplest two-level case, this first measurement of collision-induced pure dephasing rate of a molecular system provides quantitative information for understanding this elastic collision phenomenon.

II. Experimental Section

A pulsed dye laser with intracavity Etalon (Lambda Physik 2002E) pumped by an excimer laser (Lambda Physik EMG 201) was used to provide 0.06 cm⁻¹ bandwidth (fwhm) and 10 ns long pulses at 20 Hz repetition rate. The dye laser output was then doubled by a beta borium borate crystal mounted in an autotracking system (Inrad Autotracker II). Prior to intersecting the supersonic jet perpendicularly at 3 mm downstream from the pulsed nozzle with 350 μm diameter orifice, the doubled laser output was attenuated to 40 μJ per pulse to avoid saturation.

The fluorescence from the intersection region was collected vertically to the laser beam-supersonic jet plane. A pair of 2-in.-diameter *f*/1 quartz lenses placed 2 in. away from the supersonic jet were used to collect and refocus the fluorescence which was then passed through a masking slit (1 mm width) and filters (long pass from 220 nm) before being detected by a photomultiplier (Hamamatsu R2256). For the fluorescence excitation spectroscopy measurements, a boxcar (Stanford SR 250) in conjunction with a personal computer was used for processing the signal. The fluorescence decay and QB measurements were conducted using a 400 MHz transient digitizer (Tektronix TDS 380, 2 ns rise time). Each decay trace was averaged 256 times for increased *S/N* ratio.

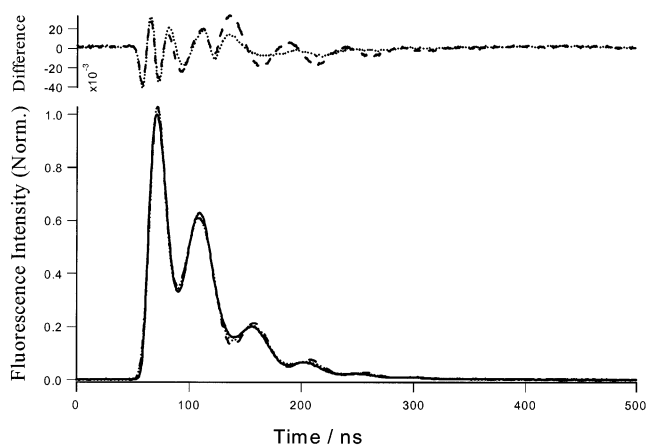


Figure 1. Fluorescence decay following the excitation of the $7_{16}(210)\tilde{C} \leftarrow 6_{15}(000)\tilde{X}$ transition of SO₂ cooled in a supersonic jet. Also shown are comparisons of the nonlinear least-squares fits with and without including collision-induced pure dephasing in QB decay. The dotted line is the fitting with pure dephasing included. The dashed line is the fitting without pure dephasing. The differences between the fitted and the experimental (solid line) curves, shown correspondingly in dotted or dashed lines, are also shown at the top of the figure.

The sample gases used for the supersonic jet were mixtures of different concentrations of SO₂ (0.1%, 0.5%, and 1.0%) seeded in He or SO₂ (0.5%) in Ar. To provide different pressures at the intersection region, different stagnation pressures (from 560 to 3200 Torr), measured by a capacitance manometer (MKS, 0–10 000 Torr range), were used.

III. Results

The fluorescence obtained after excitation of the SO₂ transition $7_{16}(210)\tilde{C} \leftarrow 6_{15}(000)\tilde{X}$ at 44861.39 cm⁻¹ is shown in Figure 1. Large amplitude modulation with only one oscillation frequency is apparent in the fluorescence decay trace. Previous study has indicated that this beat arises from the coupling between the $7_{16}(210)\tilde{C}$ rovibronic level and an isoenergetic vibrational level of the ground electronic state.^{4,5} By excitation of this transition, the single, high vibrational level 44877.52 cm⁻¹ above the zero point energy can be accessed.⁴ Rotational cooling in the supersonic expansion allows this transition to be excited without contamination from other transitions. However, as the multimode laser source is only partially coherent, the modulation depth of the beat pattern does not reach 100% despite a nearly equal mixing of the two zero-order states.^{4,36}

The collision effect on the fluorescence QB decay can be revealed in the fluorescence curves detected at the same position in the supersonic jet but with different stagnation pressures. With the increase of the stagnation pressure, the local pressure in the jet is increased and the oscillation is damped faster. Apparently, the increase of the number of collisions results in a loss of coherence and population in the excited molecular system. The following section illustrates the analysis that reveals both the collision-induced dephasing and depopulation.

IV. Analyses of Collision-Induced Fluorescence Quantum Beat Decay

A. Model. As the QB pattern shows only one oscillation frequency, the two-excited level system is used for the description of the observed QB phenomenon.^{4,5} In the coupled two level system, the two eigenstates $|1\rangle$ and $|2\rangle$ are linear combinations of the two zeroth order wave functions, a bright state $|b\rangle$

and a dark state $|d\rangle$, i.e., $|1\rangle = C_{1b}|b\rangle + C_{1d}|d\rangle$ and $|2\rangle = C_{2b}|b\rangle + C_{2d}|d\rangle$. The time evolution of the fluorescence intensity following coherent excitation of the two eigenlevels, by a partially coherent light source, can be described as³⁶

$$I(t) \propto C_{1b}^4 \exp(-\gamma_1 t) + C_{2b}^4 \exp(-\gamma_2 t) + 2\zeta |C_{1b}|^2 |C_{2b}|^2 \exp[-(\gamma_1 + \gamma_2)t/2] \cos(\omega_{12}t + \theta) \quad (1)$$

where θ is the phase difference of the two eigenstates at time $t = 0$, ω_{12} is the angular frequency corresponding to the energy difference of the two eigenstates, and γ_1 and γ_2 are the population decay rates of eigenstates $|1\rangle$ and $|2\rangle$. ζ is a coefficient depicting the effect of partial coherence in the excitation.³⁶

It has already been shown that eq 1 can be used to describe with reasonable accuracy the QB pattern and decay.^{4,5} However, eq 1 does not include the effect of collision-induced dephasing on QB decay. In principle, introducing a pure dephasing constant to the equation to describe the collision effect should improve the accuracy of the description of the QB decay if collision-induced dephasing has any discernible effect. Theoretically, it is convenient to use the density matrix method to describe the relaxation process that incorporates the effect of collision-induced dephasing.^{3,32} The time evolution of the density matrix of the system, which is embedded in a heat bath, is determined by the Liouville equation.^{3,32} In the density matrix treatment the decay of the two zero-order levels system can be described as^{14,32,33}

$$\frac{d\rho_{bb}}{dt} = -\frac{i}{\hbar}(H'_{bd}\rho_{db} - \rho_{bd}H'_{db}) - \gamma_b\rho_{bb} \quad (2)$$

$$\frac{d\rho_{dd}}{dt} = -\frac{i}{\hbar}(H'_{db}\rho_{bd} - \rho_{db}H'_{bd}) - \gamma_d\rho_{dd} \quad (3)$$

$$\frac{d\rho_{bd}}{dt} = -(i\omega_{bd} + \gamma_{bd})\rho_{bd} - \frac{i}{\hbar}H'_{bd}(\rho_{bb} - \rho_{dd}) \quad (4)$$

$$\frac{d\rho_{db}}{dt} = -(i\omega_{db} + \gamma_{db})\rho_{db} - \frac{i}{\hbar}H'_{db}(\rho_{dd} - \rho_{bb}) \quad (5)$$

Here γ_b and γ_d are the heat-bath averaged population decay rates of state $|b\rangle$ and state $|d\rangle$ respectively while γ_{bd} represents the overall dephasing constant:^{14,32,33}

$$\gamma_{bd} = \frac{1}{2}(\gamma_b + \gamma_d) + \gamma_{bd}^{(d)} \quad (6)$$

The time-dependent diagonal matrix elements ρ_{bb} and ρ_{dd} represent the population in state $|b\rangle$ and state $|d\rangle$ respectively while the off-diagonal terms ρ_{bd} and ρ_{db} are related to the coherence of the system. $\gamma_{bd}^{(d)}$ is the pure dephasing rate constant which depicts the effect of elastic collisions between the system and the heat bath. The system of interest becomes less coherent after this kind of collision: even though it does not change the energy (no depopulation), it may change the phase relationship of the excited wave functions (pure dephasing only).

Equations 2–5 cannot be solved analytically.³² In the case of biacetyl QB, Chang et al. used a numerical method to analyze the equations.¹⁴ As discussed in ref 14, if there are more than two coupled states, the zero-order basis set is preferred for the analysis. However, in the two-coupled state system, there is no difference between using the molecular eigenstates or the zero-order basis set. We note that by using the molecular eigenstates basis set the interaction between the two eigenlevels, state $|1\rangle$ and state $|2\rangle$, can be ignored and eqs 2–5 can be simplified for

analytical solutions. The notation for the equations can be changed correspondingly to the change of the basis set. The time evolution of the fluorescence intensity from the eigenlevels, following coherent excitation by a partially coherent light source, can then be described as³⁴

$$I(t) \propto C_{1b}^4 \exp(-\gamma_1 t) + C_{2b}^4 \exp(-\gamma_2 t) + 2\zeta \text{Re}\{|C_{1b}|^2 |C_{2b}|^2 \exp(-((\gamma_1 + \gamma_2)/2 + \gamma_{12}^{(d)})t) \times \exp(-i(\omega_{12}t + \theta))\} \quad (7)$$

The primary difference between eq 7 and eq 1 is the inclusion of $\gamma_{12}^{(d)}$, the pure dephasing constant of the molecular eigenstates caused by collisions, in eq 7 in the term that depicts the oscillatory pattern time evolution. In the following analysis eq 7 is used to deduce the collision pure-dephasing rate.

B. Quantum Beat Analyses. Even though previously it has been shown that eq 1 can be adequately used to extract the decay constants through a nonlinear least-squares fit of the fluorescence QB decay, the addition of a pure dephasing constant as in eq 7 does show improvement of the fitting of the QB decay. Figure 1 shows the results of the fits using both eqs 1 and 7. The laser pulse shape and detector system response, mimicked by the shape of the scattered laser pulse, have been convoluted into the fitting of the fluorescence intensity pattern. At the beginning of the fluorescence decay, there is little difference between the two fits using either eq 1 or eq 7. However, the cumulative effect of the collisions with time causes the misfit to be more apparent in the latter part of the fitting using eq 1. The fitting that includes the pure dephasing constant does provide more accurate result than the fitting without. It should be noted that both fittings resulted in coefficients $|C_{1b}|^2$ and $|C_{2b}|^2$ within the range of 0.50 ± 0.03 , in agreement with the 0.50 value determined by Xue et al. previously.⁴

The pure dephasing rate can be obtained for a particular gas mixture and stagnation pressure. The translational temperature and molecular density of the gas sample 3 mm down stream from the nozzle of that particular mixture/pressure are then deduced (see next subsection) so that the dephasing constants can be obtained and converted to cross sections.

A notable phenomenon in the QB pattern when collision-induced dephasing is occurring is the change of the oscillation frequency³³ of the QB as a function of pressure. For this reason the QB frequency was not kept constant in the fittings. Indeed this frequency shift is detected. For example, in QB decays associated with the He–SO₂(0.1%) gas mixtures the oscillation frequency shifts from 20.70 MHz at the lower pressure limit (stagnation pressure 566 Torr) to 20.02 MHz at the higher pressure limit (stagnation pressure 2360 Torr). The shift confirms the existence of pure dephasing by collision in QB. The smallness of the magnitude of the shift, 3% over a change of pressure of ~ 4 times also shows that collision-induced dephasing is relatively slow in comparison with collision-induced depopulation.

C. Modeling Collisions in the Supersonic Jet. To deduce the values of the collision-induced dephasing constant and the cross section from the measured rates, the translational velocity and the molecular density in the probe region of the supersonic jet are needed. Here, we determine the translational temperature and the molecular density through calculations using a model³⁷ built on extensive previous experimental and theoretical studies of the free jet. The details of the calculations can be found elsewhere.³⁸ In brief, to check whether the calculations are valid, the experimentally measured rotational temperature of the jet is compared with the calculated translational temperature. It is

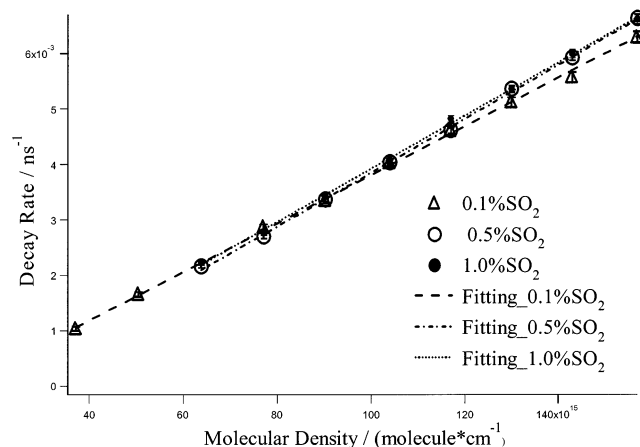


Figure 2. Stern–Volmer plot of pure dephasing rate as a function of gas density in the probe region of supersonic expansions using three types of gas mixtures: SO₂ (0.1%, 0.5%, and 1.0%) seeded in He. The different molecular densities are acquired with different stagnation pressures.

assumed here that the rotational temperature follows closely the terminal translational temperature of the expansion. The rotational temperature is obtained by fitting the laser-induced fluorescence spectra in the $\tilde{C}(210) \leftarrow \tilde{X}(000)$ transition region of SO₂ seeded in the beam. Comparisons of the two temperatures at various distances from the nozzle show that they are within 20% of each other until at least 3.5 mm away from the nozzle. With the increase of the distance away from the nozzle, both rotational and translational temperatures drop. It is anticipated that as the number of the collisions required for establishing the equilibrium between the rotational and translational degrees of freedom become less available as the local pressure decreases away from the nozzle, the difference between the two temperatures becomes larger. At the probe area 3 mm downstream from the nozzle where the fluorescence decay is measured, the calculated translational temperature is nearly identical to the measured rotational temperature and the model is used to generate the molecular density for the deduction of rate constants and cross sections in the next section.

D. Collision Dephasing Constants and Cross Sections. The pure dephasing rate $\gamma_{12}^{(d)}$ in eq 7, measured from the QB decay recorded at different stagnation pressures for the supersonic expansion, is expected to be linearly proportional to the local pressure of the bath molecules in the jet. Indeed the rate appears to be linearly increasing with the calculated local pressure in the jet, as shown in Figure 2. In this Stern–Volmer plot, the slope represents the collision-induced pure dephasing rate constant. As the pressure extrapolates to zero, the dephasing rate approaches zero, as expected. The intercept of zero dephasing rate is not at exact zero density primarily because of uncertainty in the estimate of the molecular density. Only the slope of the plot is used here for the deduction of the rate constant.

It has been previously reported that the depopulation rate of the highly excited SO₂ by collision with the ambient cold SO₂ is more than 1 order of magnitude faster than the depopulation rate by He and several times faster than that by Ar.⁴ The possibility that the dephasing rate may be much faster with SO₂ as the collider than with He and Ar suggests that we may be able to extract the dephasing rate by SO₂ collisions from the dephasing constants measured for gas mixtures with different SO₂ concentrations, even though the concentrations of SO₂ seeded in He or Ar are very low. In the case of the He supersonic expansion, the pure dephasing rate constant of excited SO₂

TABLE 1: Experimentally Determined Pure Dephasing Rate Constants and the Corresponding Cross Sections for the Three Collision Partners^a

collision partners	pure dephasing rate constant (10 ⁻¹¹ cm ³ mol ⁻¹ s ⁻¹)	calculated relative velocity (m s ⁻¹)	cross section (Å ²)
He–SO ₂ *	4.31 ± 0.08	165	26.1 ± 0.5
Ar–SO ₂ *	2.53 ± 0.05	64	39.5 ± 0.7
SO ₂ –SO ₂ *	40 ± 11	56	720 ± 190

^a The uncertainties listed for He and Ar are the 1σ values directly from the nonlinear least-squares fit. The large uncertainties in the SO₂ values reflect the small number of data points. The temperature of the probe region in the jet is calculated as 4.8 K. Also listed are the calculated relative velocities in the probe region.

(denoted as SO₂*

$$\mathbf{K}_m = \begin{pmatrix} k_1 \\ k_2 \\ k_3 \end{pmatrix} = \begin{pmatrix} 4.37 \times 10^{-11} \\ 4.68 \times 10^{-11} \\ 4.71 \times 10^{-11} \end{pmatrix} \text{cm}^3 \text{ molecule}^{-1} \text{ s}^{-1},$$

$$\mathbf{K} = \begin{pmatrix} k_{\text{SO}_2\text{-SO}_2^*} \\ k_{\text{He-SO}_2^*} \end{pmatrix}, \text{ and } \mathbf{X} = \begin{pmatrix} 0.001 & 0.999 \\ 0.005 & 0.995 \\ 0.010 & 0.990 \end{pmatrix}$$

From the matrix operations using all three k_m rate constants, the values of the pure dephasing rate constants for colliders He and SO₂ at $T = 4.8$ K are obtained. Similarly the constant for Ar can be deduced from data acquired from the SO₂ seeded in Ar jet. The pure dephasing rate constants for the three collision partners and their corresponding cross sections are listed in Table 1.

V. Discussion

In prior analysis of the SO₂ QB decay, it was assumed that the rate of pure dephasing was negligible in comparison with depopulation and the extraction of the collisional depopulation cross section can be achieved without accounting for collision-induced dephasing.⁴ This study shows that, at sufficiently high pressures, QB oscillations during the latter times of the decay curve do show a discernible effect of collision-induced dephasing. However, it is also true that the pure dephasing cross section is smaller in comparison with the depopulation cross section. In fact in all three cases the pure dephasing cross section of each collision pair is about a factor of 2 smaller than the corresponding depopulation cross section of the eigenlevels.³⁸ The depopulation cross sections obtained from the QB decay analysis without including the pure dephasing rate constant (eq 1) are very close, less than 15% deviation in numerical values, to the ones obtained from analysis with the inclusion of the pure dephasing constants (eq 7). The comparison shows that the small changes in cross sections resulted from neglecting collision dephasing in the QB decay do not change the characteristics of the previously reported depopulation cross sections.⁴

The only other reported attempt in measuring collision-induced pure dephasing in QB was for biacetyl.^{13,14} For biacetyl the QB arises as a result of singlet–triplet coupling.¹³ The earlier study¹³ indicated a large depopulation and dephasing cross

TABLE 2: Comparison of the Experimentally Obtained Pure Dephasing Cross Sections with Calculated Hard-Sphere (H-S) and Lennard-Jones (L-J) Cross Sections

collision partner	expt (\AA^2)	H-S (\AA^2)	L-J (\AA^2)	ratio expt/H-S	ratio expt/L-J
He-SO ₂ *	26	35	34	0.74	0.76
Ar-SO ₂ *	39.5	44	60	0.90	0.66
SO ₂ -SO ₂ *	722	53	87	14	8.3

section ($\sim 100 \text{\AA}^2$) caused by collisions with the bath gas. In a later study in which much narrower bandwidth excitation source and supersonic jet cooling of the sample were used,¹⁴ although no absolute value of collision cross section was obtained because the local pressure and temperature in the molecular beam were not specified, the pure dephasing rate appeared relatively smaller in comparison with the depopulation rate. This relative magnitude is consistent with our observations here.

The pure dephasing cross sections, $\sigma_{12,\text{exp}}^{(d)}$, by the three collision partners are compared with the hard sphere and Lennard-Jones³⁹ collision cross sections in Table 2. It is informative to note that the ratio of $\sigma_{12,\text{exp}}^{(d)}/\sigma_{\text{H-S}}$ increases with the complexity of the collision partner. The ratio increases by $1/3$ from He to Ar, and then much more dramatically from Ar to SO₂. The trend seems to indicate that the dephasing collision is not simply a repulsive force dominated process. Ar is more polarizable than He, and SO₂ has a permanent dipole and internal degrees of freedom. Though it is not clear from this limited set of data what molecular properties are essential for causing dephasing, if one assume that there is a significant relation between the dephasing and depopulation collisions, this trend is understandable from the fact that there is substantial long-range interaction contribution to the depopulation cross section.⁴

The implication of long-range interaction contribution to dephasing emerges even more significantly after examining the ratio of $\sigma_{12,\text{exp}}^{(d)}/\sigma_{\text{L-J}}$. The latter takes into account of the effect of the attractive potential well to the collision cross section. For He, the negligible attractive well makes the hard sphere and L-J cross sections about the same size. The much increased polarizability of Ar causes the L-J cross section to be much larger. The $\sigma_{12,\text{exp}}^{(d)}/\sigma_{\text{L-J}}$ ratios of the two noble gases are, not surprisingly, almost the same since the difference in polarizability has been taken into account into the L-J cross sections. With an increased complexity of structure and internal degrees of freedom for the SO₂ collision partner, there could be additional interaction mechanisms, such as the long-range interactions mediated through transition dipoles,^{40,41} whose effects can no longer be accounted simply by including the intermolecular energy, and the L-J cross section is no longer sufficient to describe all the long-range interaction contribution to the collision process. If this is the case, it is not surprising to see that this ratio increases dramatically from the noble gases to SO₂.

VI. Conclusion

Pressure-dependent behavior of fluorescence QB decay following the excitation of the $7_{16}(210)\bar{C} \leftarrow 6_{15}(000)\bar{X}$ transition of SO₂ at 44861.39 cm^{-1} clearly shows that pure dephasing has a discernible effect on the QB decay, particularly at the higher pressure limit. The collision-induced pure dephasing rate of the two coherently excited eigenlevels, which arises from coupling between the $\bar{C}^1\text{B}_1(210)7_{16}$ level and an isoenergetic highly vibrationally excited level 44877.52 cm^{-1} above the zero point of the electronic ground state, as well as the collision depopulation rate of the eigenlevels can be measured from the

fluorescence QB decay as a function of pressure of SO₂ seeded in a supersonic jet.

The pure dephasing collision cross sections at 4.8 K have been determined for three collision partners He, Ar and SO₂ as 26, 40, and 720\AA^2 respectively. These cross sections are all smaller than the corresponding depopulation cross sections—similar to observations made in previous studies of dephasing vs depopulation for biacetyl QB¹⁴ and of depolarization vs depopulation for NO₂ Zeeman QB.⁸ Comparisons with the hard sphere and Lennard-Jones cross sections suggest that collision-induced pure dephasing is not simply a result of repulsive hard sphere collisions.

Acknowledgment. This work is supported by the National Science Foundation, Grant No. CHE-0111520.

References and Notes

- (1) See, for example: *Highly Excited Molecule: Relaxation, Reaction, and Structure*; Mullin, A. S.; Schatz, G. C., Eds.; ACS Symposium Series 678; American Chemical Society: Washington, DC, 1997.
- (2) Parmenter, C. S. *Faraday Discuss.* **1983**, *75*, 7.
- (3) Demtröder, W. *Laser Spectroscopy*; Springer: New York, 1996.
- (4) Xue, B.; Han, J.; Dai, H. L. *Phys. Rev. Lett.* **2000**, *84*, 2606.
- (5) Ivanco, M.; Hager, J.; Sharfin, W.; Wallace, S. C. *J. Chem. Phys.* **1983**, *78*, 6531.
- (6) Watanabe, H.; Tsuchiya, S.; Koda, S. *J. Chem. Phys.* **1985**, *82*, 5310.
- (7) Brucat, P. J.; Zare, R. N. *J. Chem. Phys.* **1983**, *78*, 100.
- (8) Brucat, P. J.; Zare, R. N. *J. Chem. Phys.* **1984**, *81*, 2562.
- (9) Loge, G. W.; Tiee, J. J.; Wampler, F. B. *J. Chem. Phys.* **1986**, *84*, 3624.
- (10) Dupré, P.; Green, P. G.; Field, R. W. *Chem. Phys.* **1995**, *196*, 211.
- (11) Chang, C.; Chen, I. *J. Chem. Phys.* **2002**, *116*, 2447.
- (12) Knee, J. L.; Doany, F. E.; Zewail, A. H. *J. Chem. Phys.* **1985**, *82*, 1042.
- (13) Henke, W.; Selzle, H. L.; Hays, T. R.; Lin, S. H.; Schlag, E. W. *Chem. Phys. Lett.* **1981**, *77*, 448.
- (14) Chang, C. H.; Huang, C.; Ni, C.; Dai, H. L.; Hayashi, M.; Liang, K. K.; Kuang, A.; Chen, I. C.; Lin, S. H. *Mol. Phys.* **2002**, *100*, 1117.
- (15) Kohguchi, H.; Ohshima, Y.; Endo, Y. *Chem. Phys. Lett.* **1996**, *254*, 397.
- (16) Thoemke, J. D.; Pfeiffer, J. M.; Metz, R. B.; Crim, F. F. *J. Phys. Chem.* **1995**, *99*, 13748.
- (17) Luo, X.; Fleming, P. R.; Rizzo, T. R. *J. Chem. Phys.* **1992**, *96*, 5659.
- (18) Pack, R. T.; Butcher, E. A.; Parker, G. A. *J. Chem. Phys.* **1995**, *102*, 5998.
- (19) Furlan, A.; Scheld, H.; Huber, J. R. *J. Chem. Phys.* **1997**, *106*, 6538.
- (20) Helmer, M.; Plane, J. M. C. *J. Chem. Phys.* **1993**, *99*, 7696.
- (21) Felker, P. M.; Zewail, A. H. *J. Chem. Phys.* **1985**, *82*, 2961; *J. Chem. Phys.* **1985**, *82*, 2975; *J. Chem. Phys.* **1985**, *82*, 2994; *J. Chem. Phys.* **1985**, *82*, 3003.
- (22) Gilbert, B. D.; Parmenter, C. S.; Krajnovich, D. J. *J. Chem. Phys.* **1994**, *101*, 7423.
- (23) Clegg, S. M.; Gilbert, B. D.; Lu, S. P.; Parmenter, C. S. In ref 1, p 237.
- (24) Bouwens, R. J.; Hammerschmidt, J. A.; Grzeskowiak, M. M.; Stegink, T. A.; Yorba, P. M.; Polik, W. F. *J. Chem. Phys.* **1996**, *104*, 460.
- (25) Hamilton, C. E.; Kinsey, J. L.; Field, R. W. *Annu. Rev. Phys. Chem.* **1986**, *37*, 493.
- (26) Mordant, D. H.; Lambert, I. R.; Morley, G. P.; Ashfold, M. N. R.; Dixon, R. N.; Western, C. M.; Schnieder, L.; Welge, K. H. *J. Chem. Phys.* **1993**, *98*, 2054.
- (27) Special Issue on "Overtone Spectroscopy and Dynamics". *Chem. Phys.* **1995**, *190*.
- (28) Marcoux, P. J.; Setser, D. W. *J. Phys. Chem.* **1978**, *82*, 97.
- (29) Dai, H. L.; Field, R. W.; Kinsey, J. L. *J. Chem. Phys.* **1985**, *82*, 1606.
- (30) Dai, H. L. In *Advances in Molecular Vibrations*; Bowman, J. M., Ed.; JAI Press: Stamford, CT, 1991; p 305.
- (31) Lin, S. H.; Alden, R.; Islampour, R.; Ma, H.; Villaeys, A. A. *Density Matrix Method and Femtosecond Process*; World Scientific: Singapore, 1991.
- (32) Lin, S. H.; Eyring, H. *Proc. Natl. Acad. Sci. U.S.A.* **1977**, *74*, 3623.
- (33) Villaeys, A. A. *J. Phys. B: At. Mol. Phys.* **1983**, *16*, 3775.
- (34) Kono, H.; Fujimura, Y.; Lin, S. H. *J. Chem. Phys.* **1981**, *75*, 2569.

- (35) Golub, J. E.; Mossberg, T. W. *J. Opt. Soc. Am. B* **1986**, *3*, 554.
(36) Jiang, X. P.; Brumer, P. *Chem. Phys. Lett.* **1991**, *180*, 222.
(37) Anderson, J. B. Molecular Beam from Nozzle Sources. In *Molecular Beams and Low-Density Gas Dynamics*; Wegener, P. P., Ed.; Marcel Dekker Inc.: New York, 1974; p 1.

- (38) Han, Jun; Lee, S.; Dai, H. L. To be published.
(39) Troe, J. *J. Chem. Phys.* **1976**, *66*, 4758.
(40) Dai, H. L. In ref 1, p 266.
(41) Hartland, G. V.; Qin, D.; Dai, H. L.; Chen, C. *J. Chem. Phys.* **1997**, *107*, 2890.